AJO-DO

Influence of the hyrax expander screw position on stress distribution in the maxilla: A study with finite elements

Letícia Chaves Fernandes,[a] Robert Willer Farinazzo Vitral,[a] Pedro Yoshito Noritomi,[b] Carina Abrantes Schmitberger,[a] and Marcio José da Silva Campos[a]
Juiz de Fora, Minas Gerais, and Campinas, São Paulo, Brazil

Introduction: Our objective was to evaluate the stress and deformation distribution patterns on the maxillary bone structure using the finite element method by simulation of different vertical and anteroposterior positions of the expansion screw on the hyrax expander appliance. **Methods:** Part of the maxilla with anchorage teeth, midpalatal suture, and the hyrax appliance were modeled, and 6 distinct finite element method models were created to simulate different positions of the expansion screw. There were 2 vertical positions at distances of 20 and 15 mm from the occlusal plane. Another 3 positions were anteroposterior, with the center of the screw placed between and equidistant from the mesial face of the first molar and the distal face of the first premolar, aligned to the center of the crown of the first molar, and the anterior edge of the screw aligned to the distal face of the first molar. The initial activations of the expanders were simulated, and the stress distributions on the maxilla in each model were registered. **Results:** The stress was concentrated in the anterior region of the models, close to the incisive foramen, dissipating through the palate in the posterior and lateral orientations, in the direction of the pterygoid pillar, diverting from the midpalatal suture region. When the expander screw was simulated closer to the occlusal plane and in a more anterior position, more stress was located around the incisive foramen and distributed through the midpalatal suture to its posterior portion. More posterior positions resulted in concentrated stress around the pterygoid pillars. At all simulations, the midpalatal suture showed a V-shaped expansion, with the vertex superior in the coronal view and posterior in the axial view. **Conclusions:** Different positions of the expander screw interfered with stress intensity and distribution patterns. When the expansion screw was simulated in a more occlusal and anterior position, it was more efficient to transfer the mechanical effects from the appliance to the bone structures. (Am J Orthod Dentofacial Orthop 2019;155:80-7)

In a maxillary transverse deficiency, the maxilla has a triangular aspect, with a deep and ogival palate and constriction in the posterior segments of the dental arch, usually associated with posterior crossbite.[1-4] Rapid maxillary expansion (RME) is the standard treatment for maxillary transverse deficiency.[5,6] The orthopedic procedure uses expanders to apply lateral loads to the maxillary teeth that lead to disarticulation of the midpalatal suture (MPS) and transverse expansion of the maxilla.[7-12]

MPS disarticulation is easily obtained in children but is more difficult in patients in advanced skeletal maturation stages because of the progressive palatine suture fusion.[9] During RME, it is common to have unwanted vestibular dental inclination that compromises stability and prognosis,[7,8,13] thus limiting the orthopedic results of the treatment.[14,15]

One of the most used devices for RME is the hygienic rapid expander (hyrax), with an expander screw positioned transverse to the MPS and metallic extensions soldered to orthodontic bands in the anchorage teeth.[10-12] Variations in position of the expander screw of the hyrax expander can interfere with the load distribution of orthopedic forces,[16] influencing its efficiency and the orthopedic effect of RME.[17]

Knowledge of the effects of the expander is essential to reach the maximum potential of skeletal effects.[16] The

[a]Department of Orthodontics, Juiz de Fora Federal University, Juiz de Fora, Minas Gerais, Brazil.
[b]Renato Archer's Information Technology Center, Campinas, São Paulo, Brazil.
All authors have completed and submitted the ICMJE Form for Disclosure of Potential Conflicts of Interest, and none were reported.
Supported by Conselho Nacional de Desenvolvimento Científico e Tecnológico and Fundação de Amparo à Pesquisa de Minas Gerais.
Address correspondence to: Robert Willer Farinazzo Vitral, R 21 de Abril, 117/404, Juiz de Fora, MG 36025-090, Brazil; e-mail, robertvitral@gmail.com.
Submitted, July 2017; revised and accepted, March 2018.
0889-5406/$36.00

https://doi.org/10.1016/j.ajodo.2018.03.019

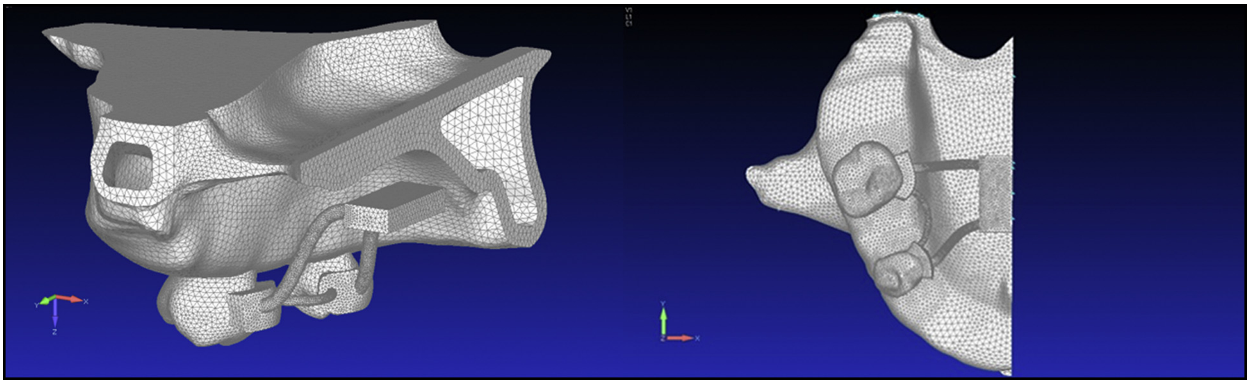

Fig 1. Mesh of tetrahedral elements in preprocessing stage.

finite element method (FEM) sets the stress and deformation states of solids subjected to external forces[18,19] and can be used in RME analysis to determine the loads and deformations to which teeth and craniofacial bones are subjected.[18,20-22]

The aim of this study was to evaluate stress and deformation distribution patterns on the maxillary bone structure using the FEM by simulation of different vertical and anteroposterior positions of the expander screw in the hyrax expander appliance.

MATERIAL AND METHODS

A finite element model from Renato Archer Technology Information Center was used for this study, and it was created from images of computed tomography (GR model Light-Speed 16 Pró) of an adult with no evident asymmetry, whose permanent teeth were all erupted except for the third molars, with no prosthetic rehabilitation and no injuries in the craniofacial region, either congenital or acquired. The use of these images to create the model was approved by the ethics research committee of the University of São Paulo (number 97/06).

A CAD model was created (Rhinoceros 4.0; McNeel North America, Seattle, Wash) from the tomography images containing the maxilla, base of the skull (zygomatic, nasal, sphenoid, and frontal bones), first premolars, and first molars on the right and left sides, and a functional bone-suture unit depicting the MPS.

The anatomic model of part of the maxilla, anchorage teeth, and MPS was imported with the software FEMAP (version 10.1.1; Siemens PLM oftware, Plano, Tx), incorporating the single-body hyrax appliance, composed of 1 expander screw and 3 wire segments with 0.036-in diameter that joined the screw to the teeth and the teeth to each other on each side, creating the geometric model with a mesh of tetrahedral elements (Fig 1).

The geometric model was subjected to a mathematical analysis in the NEI Nastran software (Noran Engineering, Westminster, Calif), using a bone thickness of 2 mm. There was a horizontal movement restriction imposed on the body of the device to simulate soldering to the orthodontic bands adapted to the teeth. The model structures were determined with specific properties (Table I), and the simulated materials had elastic, isotropic, and uniform characteristics.

Six FEM models were created to simulate different positions of the expander screw (Table II), with 3 anteroposterior and 2 vertical variations. The expander screw was positioned in the transverse center of the model's palate, perpendicular to the MPS and parallel to the occlusal plane in all simulations.

In the anteroposterior orientation (Table II; Fig 2, *A*), the center of the screw was positioned equidistant to the mesial face of the first molar and distal face of the first premolar in the anterioposterior position 1, aligned to the center of the first molar crown in the anterioposterior position 2, and in the anterioposterior position 3 the anterior edge of the expander was aligned to the distal face of the first molar. In the vertical view (Table II; Fig 2, *B*), the expander screw was positioned 20 mm (vertical position 1) and 15 mm (vertical position 2) from the occlusal plane in direction to the palate. Figure 3 shows the vertical and anteroposterior positions of all 6 models.

A condition for the outline of the maxillary bone was set for both tension distribution and displacement analysis to restrict vertical, anteroposterior, and transverse movements of the model. These conditions represented the cranial bone structures that are anatomically in contact with the maxilla, fixed in the superior (base of the skull) and posterior (pterygoid pillar) limits. A bar element was created for each node in the border of the face in the MPS and perpendicular to it. One side of the element bar was connected to the bone sharing the node with the vertex of the volumetric elements, and

Table I. Mechanical properties attributed to the structures of the geometric model

Material	*Poisson coefficient*	*Young's modulus (MPa)*
Bone[19]	0.3	10000
Teeth[23]	0.3	20000
Midpalatal suture[24]	0.49	1
Hyrax expander[19]	0.33	200000

Table II. Finite element model related to the anteroposterior and vertical positions of the expander screw

	Vertical variation	
Anteroposterior variation	*Vertical position 1*	*Vertical position 2*
Anteroposterior position 1	Model 1 (M1)	Model 4 (M4)
Anteroposterior position 2	Model 2 (M2)	Model 5 (M5)
Anteroposterior position 3	Model 3 (M3)	Model 6 (M6)

the other end was fixed (Fig 4). The activation of the hyrax was made only by the enforced displacement toward the maxillary expansion. It was possible for the model to move in the anteroposterior and vertical directions, since it can happen during hyrax activation.

In the MPS region, a mathematical condition of symmetry was imposed, and the load was symmetrically recreated on the opposite side to achieve equivalent results for both sides. In each model, a transverse displacement of 0.5 mm in the center of the screw was simulated; because of the symmetry condition, this was equivalent to a 1-mm activation of the hyrax expander.

RESULTS

The numbers of nodes and elements of the mesh in each model were different due to the length variations in the arms of the expander screw (Table III).

For the transverse displacement of the maxilla, after simulating the screw opening, all models had a V-shaped expansion, with a superior and posterior vertex, with a greater opening in the alveolar region in the coronal view (Fig 5, *A*) and the anterior region, close to the incisive foramen in the axial view (Fig 5, *B*). These images used a rendering of the bar elements in a 100:1 scale to highlight and facilitate visualizing how the system behaves.

For the evaluation of stress distribution, the stress in the model M1 (Fig 6) was concentrated in the anterior region, close to the incisive foramen, with maximum tension about 15 MPa, coinciding with the region of greater transverse opening. The stress dissipated through the palate anteroposteriorly, directed to the pterygoid bone, deviating from the MPS region. This stress distribution pattern was found in all models, differing in the intensity of maximum tension.

Model M2 (Fig 6) showed lower stress in all regions. The incisive foramen had the highest stress in the model, approximately 9 MPa.

In model M3 (Fig 6), the maximum stress was lower around the incisive foramen—approximately 7.5 MPa—with an increase of stress intensity distributed from the anterior to the posterior directions. In this model, the region of highest stress changed and was observed around the pterygoid bone.

Model M4 (Fig 6) had the largest area of stress distribution and the highest levels of stress, with values above 30 MPa registered in the regions of the incisive foramen and pterygoid bone. In this model, the stress distribution reached the central region of the palate.

Model M5 (Fig 6) showed similar areas of stress distribution to model M4, including the MPS region, although with lower levels of stress.

In model M6 model (Fig 6), there was minor stress distribution, similar to M3, but with even less intensity. The maximum stress in the model (approximately 9 MPa) was registered in the posterior region, and the region of the incisive foramen showed maximum values about 5.5 MPa, the lowest in the models.

The analysis of the maxilla from the median palatine suture from the sagittal or internal cut view (Fig 7) agrees with the data in the occlusal (axial) views, with the same stress distribution tendencies in the median palatine suture. Models 4, 5, and 6 showed the greatest areas, in decreasing order, of stress dissipation in the region of the suture.

DISCUSSION

RME is a common treatment for skeletal maxillary transverse deficiency.[20] The loads and deformations to which teeth and craniofacial bones are subjected in this procedure have been analyzed with good results by the FEM.[20,22,25]

In this study, the properties for the behavior of different structures in the model (Young's modulus and Poisson's ratio) were set independently from the patients' ages.[23,24,26,27] In addition, to evaluate the structures' displacements after opening the expander screw, bar elements were used in the MPS, simulating the elastic properties presented by this structure in individuals during growth, prone to MPS disarticulation.

The position of the expander screw is not rigidly determined in the design of the expander appliance, since it varies according to the experience of the practitioner.[16] With the finite element model, Araugio et al[16] evaluated the degree of dental inclination during

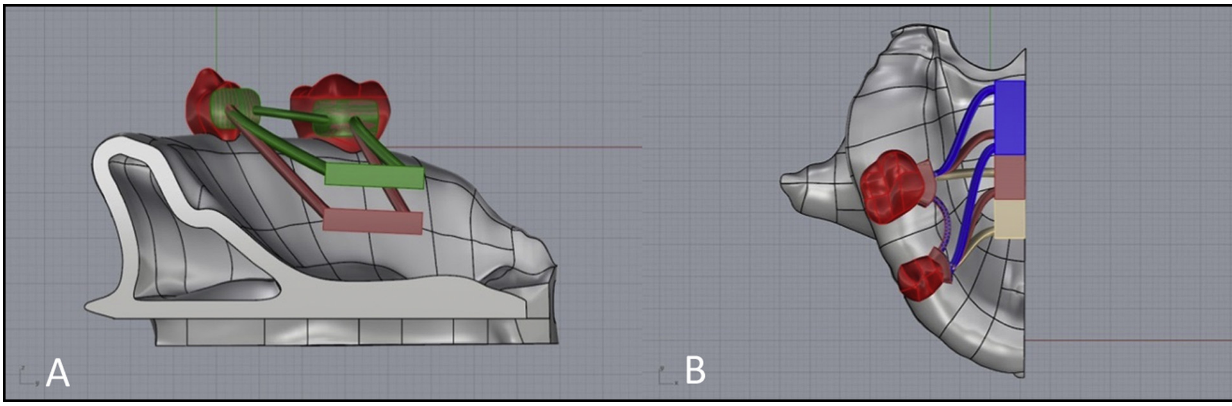

Fig 2. A, Anteroposterior and **B,** vertical positions of the expander screw.

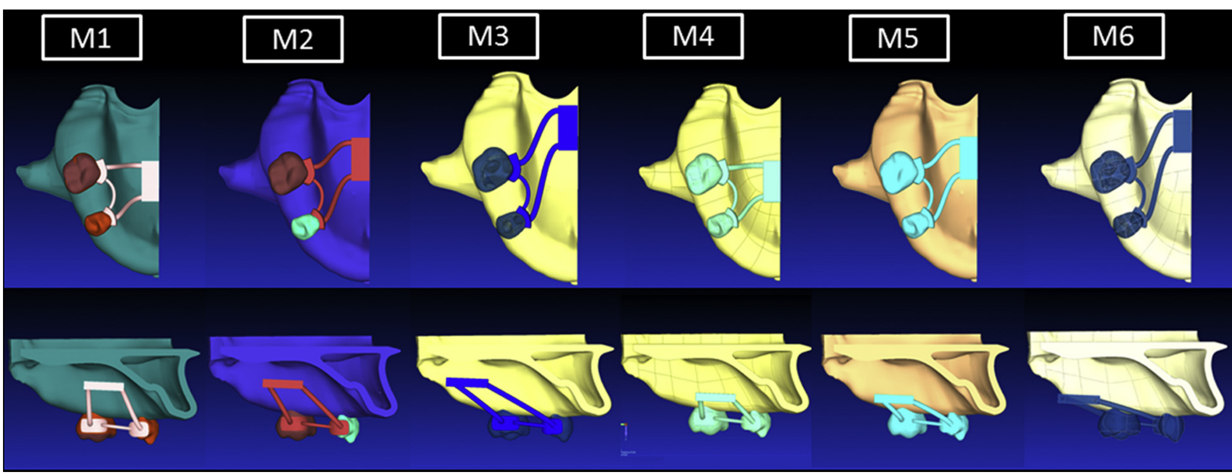

Fig 3. Axial and sagittal views of the anteroposterior and vertical positions of the 6 models.

RME with different heights of the expander screw, but they did not consider anteroposterior variations of the expander screw, and it did not describe load distributions on bone structures.

The study and improvement of expander appliances aim not only to minimize unwanted tooth displacement, but mostly to maximize orthopedic effects.[16,28,29] These effects are related to the capacity of expander appliances to impose optimal transverse loads to the maxilla, which can be simulated in a computational model by the FEM.[28,30] An effective load distribution during MPS opening is related to a lower residual tension at the end of the activation period, reducing the amount of time required for bone remodeling in the stabilization phase.[17]

In general, we found that the tensions were concentrated in the anterior portion of the models, close to the incisive foramen, dissipating through the palate in a posterior and lateral direction, toward the pterygoid pillars—another area of stress concentration, as described by Matsuyama et al.[31] Liu et al[17] described the stress accumulation in the anterior region on the first stages of activation of the expander screw as a factor that helps in the initial opening of the MPS. After overcoming the first resistance of the MPS, the opening pattern behaved the same way in all models in this study, with a superior and posterior vertex, as already described in the literature.[19,22,31-36] This pyramidal pattern of expansion can be due to the different levels of resistance of the MPS along its length and to the presence of the pterygomaxillary structure, which limits its expansion.[31]

The vertical and anteroposterior variations of the expander screw resulted in different stress distributions

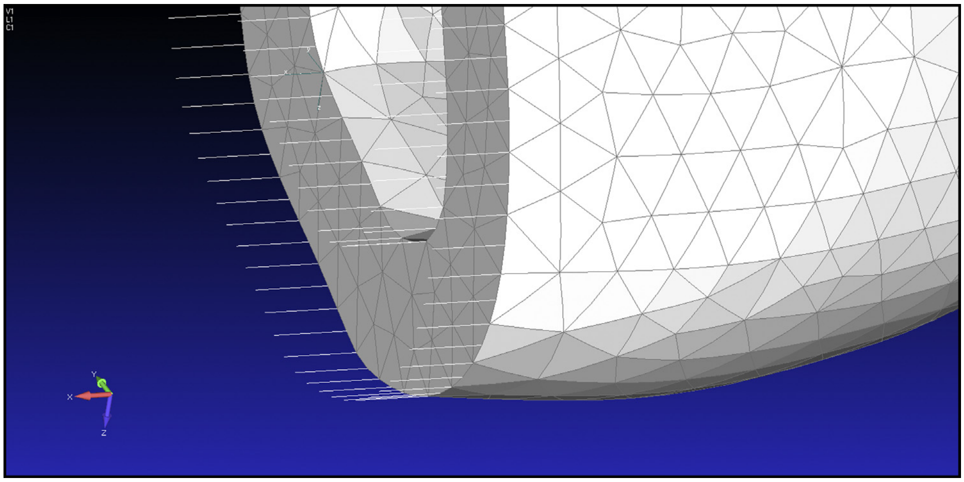

Fig 4. Bar elements connection.

Table III. Number of nodes and elements of the mesh in each model

Model	*Numbers of nodes*	*Elements of the mesh*
M1	452775	298716
M2	585703	388772
M3	646482	426757
M4	405764	267517
M5	434441	286567
M6	451859	297940

in the maxilla. When in the more anterior positions, P1 and P2, there was a highest load transfer from the expander screw to the bone structures after activating the appliance, with bigger areas of stress distribution and higher levels of stress through the maxilla. Models M4 and M5 were the only ones in which the stress reached the posterior portion of the MPS.

The simulations of the anteroposterior position P3 (models M3 and M6) showed stress concentrations close to the pterygoid pillar, where we also noted the highest stress level. The maxilla in this region is more resistant to lateral openings, making the stress concentration ineffective to promote RME.[31] This change in the stress distribution pattern could be related to the greater anteroposterior misalignment of the expander screw with the point of application of force (molars and premolars); this leads to higher energy consumption by the appliance in the moment of activation, due to the flexibility of the appliance and the reduction of load intensity along the maxilla.

Regarding the vertical position, when the expander screw was placed closer to the occlusal plane, there was a more efficient conversion from the mechanical effect of the screw opening to stress on the bone structures, probably associated with the shorter length of the arms of the device, and because the expander screw was vertically closer to the center of resistance of the teeth.[16] Therefore, apart from the models with the expander screw in the most posterior position (M3 and M6), those with the expander screw in the occlusal position (M4 and M5) had more extensive areas of stress distribution and higher levels of stress than did the models with the expander screw in the cervical position (M1 and M2).

Although the vertical position of the expander screw showed greater influence in stress distribution and intensity than did the anteroposterior variation, the model with the most favorable results (M4) and the model with the least favorable results (M6) were in the same vertical position, in the farthest anterior and posterior positions, respectively. The expander screw had better results in the most anterior and occlusal position; thus, the M4 model was the most efficient. Comparatively, the M6 model (the most posterior and occlusal) was the one that transferred the lowest loads to the bone structure after activation.

In the models simulated, the most occlusal position of the expander screw allowed for a better stress distribution in the maxilla after the hyrax expander was activated. Although the expander screw was associated with an increase in the patient's discomfort when it was closer to the occlusal plane,[37] the stage of active treatment with this device is fairly short. More comfortable retention devices can be used after the expected result is reached.

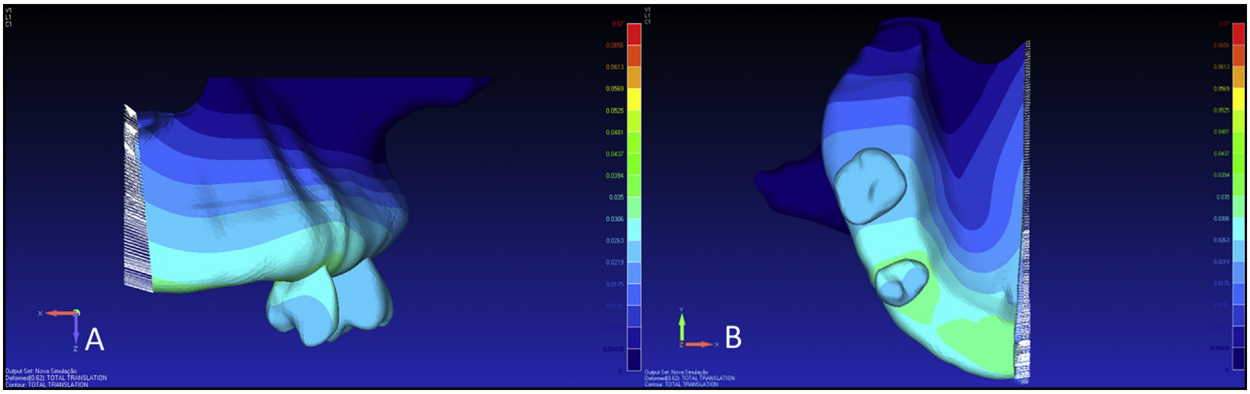

Fig 5. Displacement in the **A,** coronal plane and **B,** axial plane; scale 100:1.

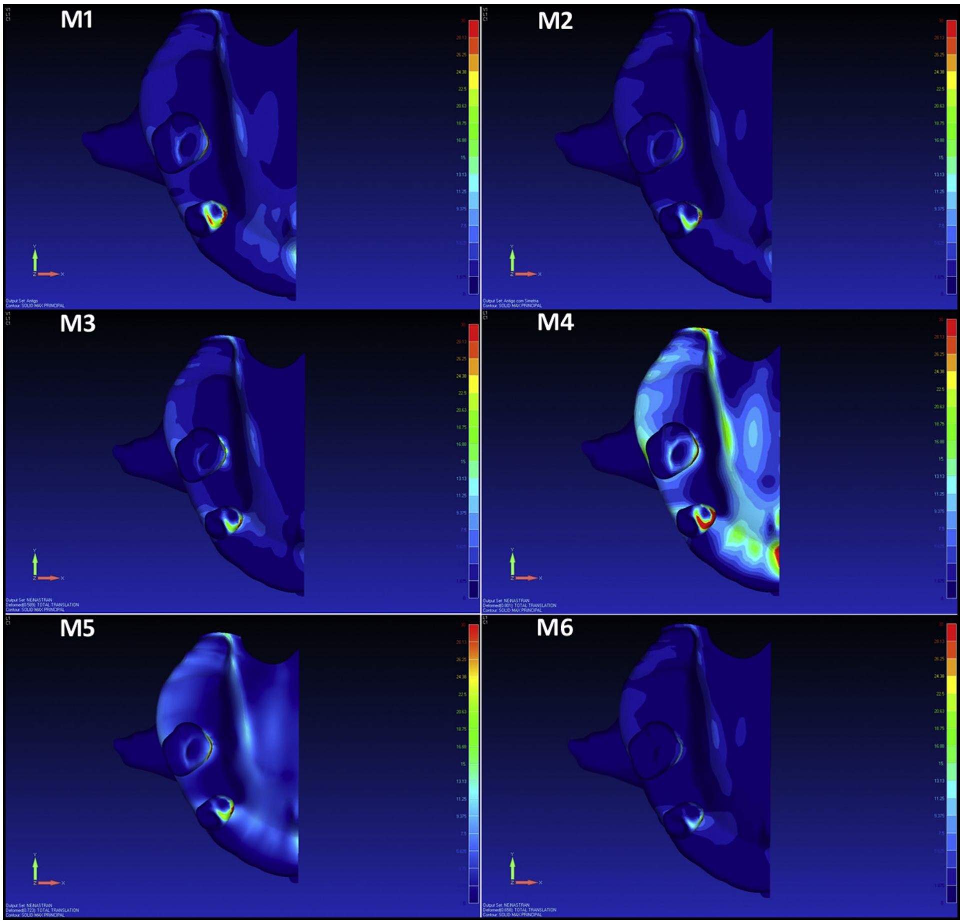

Fig 6. View in the axial plane of maximum tension in all 6 models. The images show the tension in megapascals distributed along the maxilla in each model, with color variations from blue to red for lower and higher tensions, respectively.

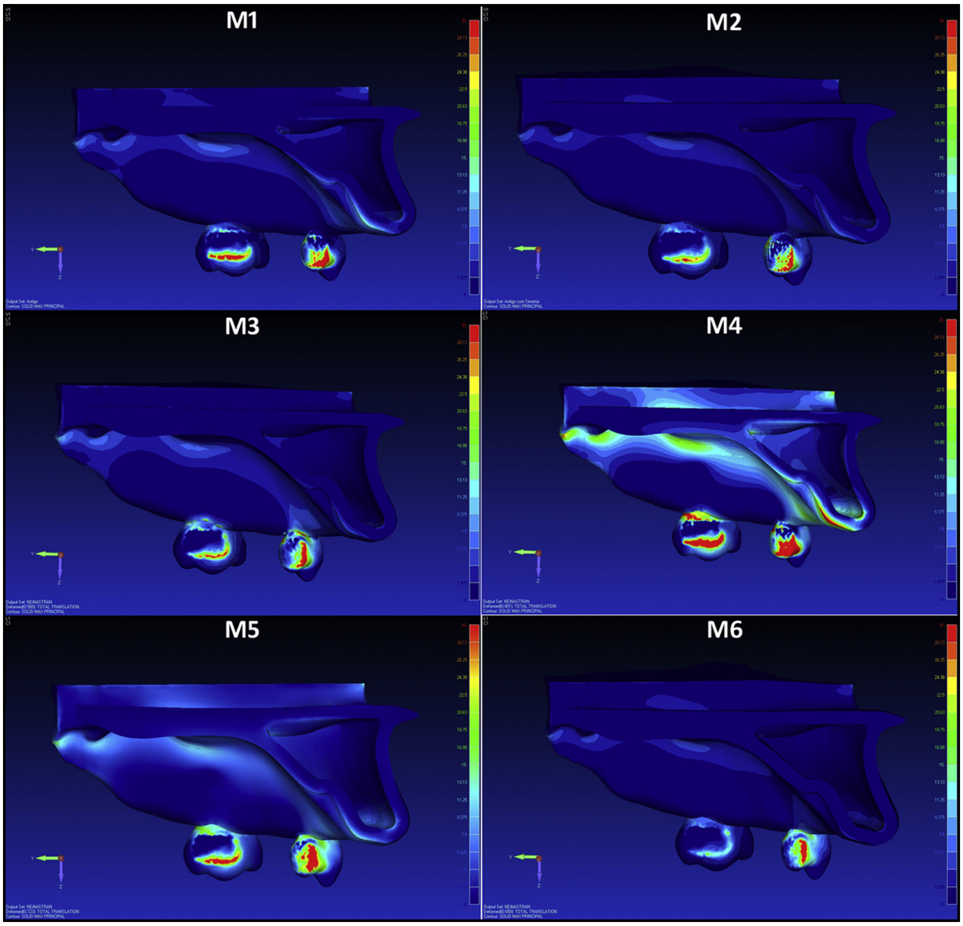

Fig 7. View in the sagittal plane (MPS) of maximum tension in all 6 models. The images show the tension in megapascals distributed along the maxilla in each model, with color variations from blue to red for lower and higher tensions, respectively.

CONCLUSIONS

The simulations of activation of the expander screw in different positions with the FEM showed the following.

1. There was a V-shaped expansion in the maxilla, with a superior and posterior vertex, in every position of the expander screw.
2. Variations in the positions of the expander screw in the vertical and anteroposterior directions interfered with the patterns of distribution and the intensity of stress. The anteroposterior variation had the most influence.
3. The most occlusal and anterior position of the screw was more effective to transfer the mechanical effects from the expander to the bone structures, with a larger area of stress distribution and higher stress values in the maxilla.

REFERENCES

1. Haas AJ. Rapid expansion on the maxillary dental arch and nasal cavity by opening the midpalatal suture. Angle Orthod 1961;31:73-90.
2. Haas AJ. Long-term posttreatment evaluation of rapid palatal expansion. Angle Orthod 1980;50:189-217.
3. McNamara JA. Maxillary transverse deficiency. Am J Orthod Dentofacial Orthop 2000;117:567-70.
4. Garrett BJ, Caruso JM, Rungcharassaeng K, Farrage JR, Kim JS, Taylor GD. Skeletal effects to the maxilla after rapid maxillary expansion assessed with cone-beam computed tomography. Am J Orthod Dentofacial Orthop 2008;134:8-11.
5. Haas AJ. The treatment of maxillary deficiency by opening the midpalatal suture. Angle Orthod 1965;35:200-17.
6. Knaup B, Yildizhan F, Wehrbein H. Age-related changes in the midpalatal suture. A histomorphometric study. J Orofac Orthop 2004;65:467-74.
7. Starnbach HK, Cleall JF. The effects of splitting the midpalatal suture on the surrounding structures. Am J Orthod 1964;50:923-4.
8. Starnbach H, Bayne D, Cleall J, Subtelny JD. Facioskeletal and dental changes resulting from rapid maxillary expansion. Angle Orthod 1966;36:152-64.

9. Podesser B, Williams S, Crismani AG, Bantleon HP. Evaluation of the effects of rapid maxillary expansion in growing children using computer tomography scanning: a pilot study. Eur J Orthod 2007; 29:37-44.
10. Biederman W. A hygienic appliance for rapid expansion. J Pract Orthod 1968;2:67-70.
11. Chaconas SJ, Caputo AA. Observation of orthopedic force distribution produced by maxillary orthodontic appliances. Am J Orthod Dentofacial Orthop 1982;82:492-501.
12. Garib DG, Henriques JF, Janson G, Freitas MR, Coelho RA. Rapid maxillary expansion—tooth tissue-borne versus tooth-borne expanders: a computed tomography evaluation of dentoskeletal effects. Angle Orthod 2005;75:548-57.
13. Mew J. Relapse following maxillary expansion: a study of twenty-five consecutive cases. Am J Orthod 1983;83:56-61.
14. Haas AJ. Palatal expansion: just the beginning of dentofacial orthopedics. Am J Orthod 1970;57:219-55.
15. Haas AJ. Rapid palatal expansion: a recommended prerequisite to Class III treatment. Trans Eur Orthod Soc 1973;311-8.
16. Araugio RM, Silva JD, Pacheco W, Pithon MM, Oliveira DD. Influence of the expansion screw height on the dental effects of the hyrax expander: a study with finite elements. Am J Orthod Dentofacial Orthop 2013;143:221-7.
17. Liu S, Xu T, Zou W. Effects of rapid maxillary expansion on the midpalatal suture: a systematic review. Eur J Orthod 2015;37: 651-5.
18. Lee H, Ting K, Nelson M, Sun N, Sung SJ. Maxillary expansion in customized finite element method models. Am J Orthod Dentofacial Orthop 2009;136:367-74.
19. Serpe LC, Las Casas EB, Toyofuku AC, Gonzalez-Torres LA. A bilinear elastic constitutive model applied for midpalatal suture behavior during rapid maxillary expansion. Res Biomed Eng 2015;31:319-27.
20. Han UA, Kim Y, Park JU. Three-dimensional finite element analysis of stress distribution and displacement of the maxilla following surgically assisted rapid maxillary expansion. J Craniomaxillofac Surg 2009;37:145-54.
21. Jafari A, Shetty KS, Kumar M. Study of stress distribution and displacement of various craniofacial structures following application of transverse orthopedic forces—a three-dimensional FEM study. Angle Orthod 2003;73:12-20.
22. Provatidis CG, Georgiopoulos B, Kotinas A, McDonald JP. Evaluation of craniofacial effects during rapid maxillary expansion through combined in vivo/in vitro and finite element studies. Eur J Orthod 2008;30:437-48.
23. Serpe LC, Torres LA, de Freitas Pinto RU, Toyofuku AC, de Las Casas EB. Maxillary biomechanical study during rapid expansion treatment with simplified model. J Med Imaging Health Inform 2014;4:137-41.
24. Tanne K, Hiraga J, Sakuda M. Effects of directions of maxillary protraction forces on biomechanical changes in craniofacial complex. Eur J Orthod 1989;11:382-91.
25. Gautam P, Zhao L, Patel P. Biomechanical response of the maxillofacial skeleton to transpalatal orthopedic force in a unilateral palatal cleft. Angle Orthod 2011;81:503-9.
26. Hibbeler RC. Mechanics of materials. 5th ed. Uppler Saddle Riverk, NJ: Prentice Hall; 2002.
27. Wang Q, Wood AS, Grosse IR, Ross CF, Zapata U, Byron CD, et al. The role of the sutures in biomechanical dynamic simulation of a macaque cranial finite element model: implications for the evolution of craniofacial form. Anat Rec 2012;295:278-88.
28. Trindade IE, Castilho RL, Sampaio-Teixeira AC, Trindade-Suedam IK, Silva-Filho OG. Effects of orthopedic rapid maxillary expansion on internal nasal dimensions in children with cleft lip and palate assessed by acoustic rhinometry. J Craniofac Surg 2010;21:306-11.
29. Goldenberg DC, Goldenberg FC, Alonso N, Gebrin ES, Amaral TS, Scanavini MA, et al. Hyrax appliance opening and pattern of skeletal maxillary expansion after surgically assisted rapid palatal expansion: a computed tomography evaluation. Oral Surg Oral Med Oral Pathol Oral Radiol Endod 2008;106:812-9.
30. Ghoneima A, Abdel-Fattah E, Hartsfield J, El-Bedwehi A, Kamel A, Kula K. Effects of rapid maxillary expansion on the cranial and circummaxillary sutures. Am J Orthod Dentofacial Orthop 2011; 140:510-9.
31. Matsuyama Y, Motoyoshi M, Tsurumachi N, Shimizu N. Effects of palate depth, modified arm shape, and anchor screw on rapid maxillary expansion: a finite element analysis. Eur J Orthod 2015;37:188-93.
32. Wertz RA. Skeletal and dental changes accompanying rapid midpalatal suture opening. Am J Orthod 1970;58:41-66.
33. Timms DJ. A study of basal movement with rapid maxillary expansion. Am J Orthod 1980;77:500-7.
34. Davidovitch M, Efstathiou S, Sarne O, Vardimon AD. Skeletal and dental response to rapid maxillary expansion with 2-versus 4-band appliances. Am J Orthod Dentofacial Orthop 2005;127: 483-92.
35. Lione R, Ballanti F, Franchi L, Baccetti T, Cozza P. Treatment and posttreatment skeletal effects of rapid maxillary expansion studied with low-dose computed tomography in growing subject. Am J Orthod Dentofacial Orthop 2008;134:389-92.
36. Weissheimer A, Menezes LM, Mezomo M, Dias DM, Lima EM, Rizzatto SM. Immediate effects of rapid maxillary expansion with Haas-type and hyrax-type expanders: a randomized clinical trial. Am J Orthod Dentofacial Orthop 2011;140:366-76.
37. De Felippe NL, Da Silveira AC, Viana G, Smith B. Influence of palatal expanders on oral comfort, speech, and mastication. Am J Orthod Dentofacial Orthop 2010;37:48-53.